AMERICAN SOCIETY of
GENE & CELL
THERAPY

# A Genetically Engineered Primary Human Natural Killer Cell Platform for Cancer Immunotherapy

Emily J. Pomeroy,[1,2,3] John T. Hunzeker,[1,2,3] Mitchell G. Kluesner,[1,2,3] Walker S. Lahr,[1,2] Branden A. Smeester,[1,2,3] Margaret R. Crosby,[1,2] Cara-lin Lonetree,[1,2,3] Kenta Yamamoto,[1] Laura Bendzick,[5] Jeffrey S. Miller,[4] Melissa A. Geller,[2,5] Bruce Walcheck,[6] Martin Felices,[2,4] Beau R. Webber,[1,2,3] Timothy K. Starr,[2,3,5] and Branden S. Moriarity[1,2,3]

[1]Department of Pediatrics, University of Minnesota, Minneapolis, MN 55455, USA; [2]Masonic Cancer Center, University of Minnesota, Minneapolis, MN 55455, USA; [3]Center for Genome Engineering, University of Minnesota, Minneapolis, MN 55455, USA; [4]Department of Medicine, Division of Hematology, Oncology, and Transplantation, University of Minnesota, Minneapolis, MN 55455, USA; [5]Department of Obstetrics, Gynecology, and Women's Health, University of Minnesota, Minneapolis, MN 55455, USA; [6]Department of Veterinary and Biomedical Sciences, University of Minnesota, Saint Paul, MN 55455, USA

**Enhancing natural killer (NK) cell cytotoxicity by blocking inhibitory signaling could lead to improved NK-based cancer immunotherapy. Thus, we have developed a highly efficient method for editing the genome of human NK cells using CRISPR/Cas9 to knock out inhibitory signaling molecules. Our method efficiently edits up to 90% of primary peripheral blood NK cells. As a proof-of-principle we demonstrate highly efficient knockout of *ADAM17* and *PDCD1*, genes that have a functional impact on NK cells, and demonstrate that these gene-edited NK cells have significantly improved activity, cytokine production, and cancer cell cytotoxicity. Furthermore, we were able to expand cells to clinically relevant numbers, without loss of activity. We also demonstrate that our CRISPR/Cas9 method can be used for efficient knockin of genes by delivering homologous recombination template DNA using recombinant adeno-associated virus serotype 6 (rAAV6). Our platform represents a feasible method for generating engineered primary NK cells as a universal therapeutic for cancer immunotherapy.**

## INTRODUCTION

Natural killer (NK) cells are a critical component of the innate immune system due to their ability to kill a variety of target cells, including cancer cells. NK cell cytotoxicity is mediated by the integration of signals from activating and inhibitory receptors and cytokines.[1] The ability of NK cells to kill tumor cells, along with the ease with which they are isolated and expanded from peripheral blood, has made them an attractive source for immunotherapy.[2,3] Moreover, because NK cells do not induce graft-versus-host disease,[4] they can be generated from unrelated donors and, therefore, represent a potential "off-the-shelf" therapeutic product. However, NK cell immunotherapy has seen limited success in the clinic, due in part to lack of persistence and expansion after transplant.[5] Changes in NK cell receptor repertoire and ligand expression in the tumor microenvironment can also lead to decreased NK cell activity.[6,7] Thus, it is predicted that targeting the receptor repertoire, specifically by decreasing inhibitory signals imposed upon NK cells, may lead to enhancement of their anti-tumor activity.[8] To date, multiple phase I and phase II clinical trials testing NK cell checkpoint blockade against KIR (ClinicalTrials.gov: NCT01714739 and NCT01750580) and NKG2A (ClinicalTrials.gov: NCT02331875) as a therapy for hematological and solid tumors are ongoing.

One of the most potent activating receptors on NK cells is CD16a (Fc-gamma receptor IIIa [FcγRIIIa]). This Fc receptor binds the Fc portion of immunoglobulin G (IgG)-coated target cells and induces antibody-dependent cell-mediated cytotoxicity (ADCC), which is a key molecular mechanism of several clinically successful anti-tumor therapeutic monoclonal antibodies (mAbs).[9,10] After activation, CD16a is rapidly cleaved from the cell surface by A Disintegrin And Metalloproteinase-17 (ADAM17).[11] Inhibition of ADAM17 leads to increased cytokine production by human NK cells,[12] suggesting that the use of tumor-targeting mAbs combined with inhibition of ADAM17 could enhance the anti-tumor response.

Various cells within the tumor micro-environment express immunosuppressive molecules that interfere with the complex array of receptors that regulate NK cells and their ability to expand.[13] For example, some tumor cells upregulate PD-L1, which engages PD1 on NK cells, reducing cytotoxic activity.[14,15] This inhibition imposed on NK cells limits effective NK immunotherapy, and overcoming this immunosuppression could improve therapeutic development. Strategies for overcoming these challenges have focused on releasing NK cell inhibition through the use of small-molecule inhibitors and mAbs.[16–18] However, there are limitations to these strategies: off-target toxicity is common with these types of therapies, and importantly, no
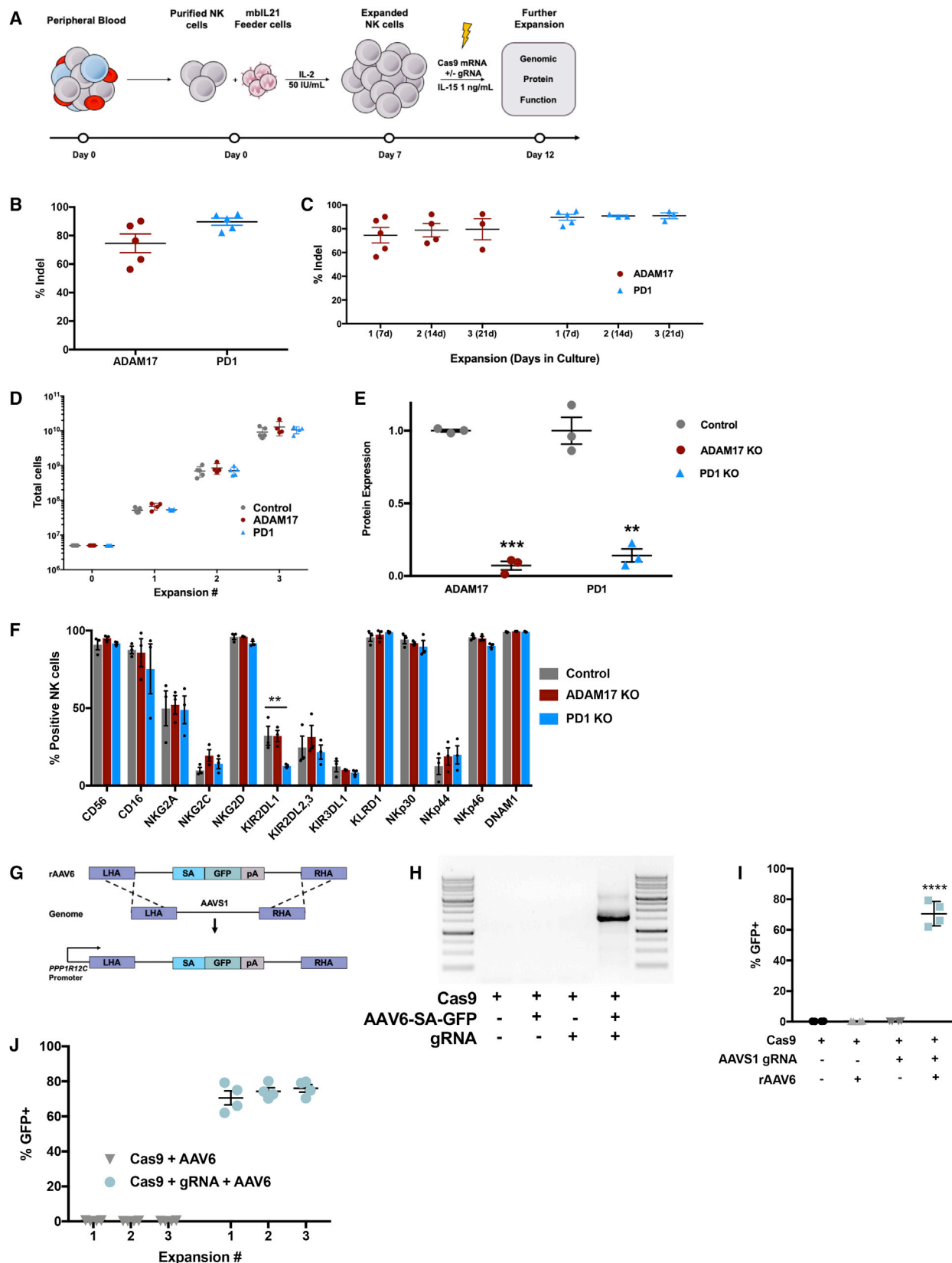
humanized antibodies or chemical inhibitors exist for some high-interest targets.

An alternative approach is to use CRISPR/Cas9 to edit genes relevant to NK function in order to improve their utility as an immunotherapeutic agent. Changes made with this approach are confined to NK cells, reducing undesirable systemic effects. Additionally, design and optimization of CRISPR guide RNAs (gRNAs) are straightforward and cost-effective, making it easy to target any gene of interest. Here, we present a method for achieving high rates of gene editing in activated primary human NK cells. We can expand edited NK cells to clinically relevant numbers and demonstrate that gene-edited NK cells have enhanced function *in vitro* and *in vivo*. Our method is capable of knocking out genes at rates up to 90% and site-specifically knocking in genes at rates approaching 80%. In summary, we present a rapid platform for generating high-functioning genetically modified NK cells for use in cancer immunotherapy.

## RESULTS

### A Platform for Efficient Gene Editing of Primary Human NK Cells

To improve NK cell cytotoxicity, we developed an optimized CRISPR/Cas9 system capable of disrupting important regulatory genes in activated primary human NK cells. Based on our previous work with primary human T cells and B cells,[19,20] we hypothesized that activating NK cells prior to electroporation would make them more amenable to nucleic acid delivery. We delivered nucleic acid in the form of EGFP mRNA to NK cells isolated from peripheral blood mononuclear cells (PBMCs) activated with irradiated feeder cells expressing membrane-bound interleukin (IL)-21 (Clone9.mbIL21 [C9])[21] and cultured with IL-2 for 7 days prior to electroporation (Figure 1A). Using this approach, we routinely achieve >98% transfection efficiency with >90% cell viability (Figure S1A). Although other feeder cell and feeder cell-free expansion methods exist, we chose to use C9 feeder cells to activate and expand NK cells because this method has been shown to be safe and effective in patients with multiple myeloma.[22] However, the effectiveness of CRISPR editing is based on the activation state of the NK cells, and thus our electroporation parameters could be used with NK cells expanded using different methods (unpublished data).

To test our optimized protocol, we delivered Cas9 mRNA alone as a control or in combination with chemically modified gRNAs[23] target-ing *ADAM17*[24] or *PDCD1*[15] to activated NK cells from five independent human donors. Next generation sequencing (NGS) of amplified target regions revealed gene-editing efficiency of 80.9% ± 9.9% for *ADAM17* and 81.9% ± 7.4% for *PDCD1* without the use of any enrichment methods (Figure 1B). The differences in editing efficiency at the chosen target sites are attributed to efficiency of the specific gRNA and accessibility of the target locus.[25] We compared NGS and Tracking of Indels by Decomposition (TIDE) analysis to quantify gene-editing efficiency in all samples. The TIDE web tool quantifies indel formation using Sanger sequencing reactions.[26] We observed no significant difference between editing efficiency calculated using TIDE versus NGS, in line with previous reports[27] (Figure S1B), and as such we used TIDE for all further analysis of gene editing.

### Gene-Edited NK Cells Can Be Expanded to Clinically Relevant Numbers

The dose of infused NK cells in the clinical setting ranges from $1 \times 10^6$ to $1 \times 10^8$ cells/kg.[28] Thus, a typical patient would require ~$8 \times 10^9$ NK cells at a high dose. Critically, we were able to maintain the gene edits at similar frequencies after multiple rounds of expansion during 21 days of culture using C9 feeder cells (Figure 1C), and gene knockout (KO) did not affect our ability to expand cells to the clinically relevant numbers referenced above (Figure 1D).

### Protein Expression Is Significantly Altered in Gene-Edited Cells and Minimal Off-Target Activity Is Detected

Protein expression of targeted genes was significantly decreased (89.8% ± 1.2% for ADAM17 and 86.9% ± 7.8% for PD1), and mRNA expression followed a similar pattern (Figure 1E; Figures S1C–S1F). To assess clinical safety, the top 10 putative off-target sites for each gRNA were computationally identified and analyzed for off-target editing. NGS showed no indel formation at any of the predicted off-target sites (Figure S1G). Furthermore, with the goal of developing clinical products, we sought to optimize cryopreservation of activated and gene-edited NK cells. Previous groups have shown low NK cell recovery after cryopreservation.[29] We found that freezing $1 \times 10^7$ NK cells/mL using CryoStor CS10 preservation media yielded ~80% recovery after thaw, and that gene editing did not affect this process (Figure S1H). The use of C9 feeder cells has been shown to maintain integrity of the NK cell receptor repertoire.[21] We compared expression of 13 NK cell receptors in control and CRISPR-edited samples

---

**Figure 1. A Highly Efficient Method of CRISPR/Cas9-Based Engineering of Primary Human NK Cells**

(A) Protocol for expansion and gene editing of primary human NK cells. In brief, NK cells are isolated from PBMCs of healthy human donors and co-cultured for 1 week with mbIL21 (C9) feeder cells in the presence of IL-2. Expanded NK cells are electroporated with Cas9 mRNA alone (control) or in combination with gRNA targeting a gene of interest. Electroporated NK cells are recovered in media containing IL-15 and then analyzed for genomic editing, protein loss, and function. (B) Next generation sequencing (NGS) analysis of indel formation after delivery of Cas9 mRNA + gRNA targeting ADAM17 (maroon) and PD1 (blue) (n = 5 independent donors). (C) Analysis of indel formation by TIDE over serial expansions with C9 feeder cells: x axis shows expansion number and total days in culture (n = 5 independent donors). (D) Expansion of engineered cells to clinically relevant numbers using multiple rounds of C9 expansion (n = 5 independent donors). (E) Protein expression in knockout NK cells (colored bars) compared with control cells (gray bars) normalized to 1. Flow cytometry analysis of % ADAM17+ NK cells (maroon, n = 3 independent donors, ***p = 0.0002, Student's t test), and flow cytometry analysis of % PD1+ NK cells normalized to controls (blue, n = 3 independent donors, **p = 0.0011, Student's t test) after gene knockout. (F) Expression of a panel of NK cell markers measured by flow cytometry in control or gene-modified NK cells (n = 3 independent donors). (G) Gene knockin strategy to integrate a splice-acceptor-EGFP cassette to the AAVS1 locus using rAAV6 and CRISPR/Cas9. (H) PCR primers were designed to span and amplify the 3′ junction of genomic AAVS1 and EGFP. (I) EGFP expression 14 days after gene knockin with rAAV6 (n = 4 independent donors, ****p = 0.0016, Student's t test). (J) EGFP expression after three rounds of expansion with C9 feeder cells.

(Figure 1F; Figure S2A). Although we found a reduction in KIR2DL1 expression in PD1 KO NK cells and some donor variability in expression of CD16a, KIR2DL2,3, and KIR3DL1, overall expression levels were very similar in control and engineered cells.

### Efficient Targeted Gene KI Using Adeno-Associated Virus

In addition to successful gene KO, we adapted our method for gene knockin (KI) by co-delivering a DNA template for homologous recombination (HR) using recombinant adeno-associated virus serotype 6 (rAAV6), along with Cas9 mRNA and gRNA. This approach has been used to achieve targeted integration of a transgene in primary human T cells and CD34^{+} hematopoietic stem cells.[30] This method has advantages over conventional delivery of a transgene using lentiviral-based methods, including maintenance of endogenous regulatory elements at the site of integration and preclusion of deleterious effects due to insertional mutagenesis.[31] As proof-of-principle, we delivered Cas9 and gRNA targeting the AAVS1 safe harbor locus downstream of the endogenous promoter-splice donor (Figure 1G). Co-delivery of a promoter-less EGFP targeting vector using rAAV6 resulted in successful HR in 75.6% ± 3.0% of NK cells based on junction PCR and EGFP expression (Figures 1H and 1I). Similar to gene KO, gene KI was stable through several rounds of expansion using C9 feeder cells (Figure 1J). Together, these data demonstrate that high-efficiency Cas9-mediated gene KO and KI are achievable in activated primary human NK cells.

### KO of ADAM17 or Modification of CD16 Can Prevent CD16 Shedding and Enhance ADCC

ADAM17 is responsible for the rapid cleavage of the activating FcγRIIIa (CD16a) from the surface of NK cells after activation,[11,24,32] resulting in temporary inhibition ADCC events and the ensuing NK cytotoxicity. Small-molecule inhibitors of ADAM17 are currently in clinical trials in combination with antibody treatments as a method of enhancing the therapeutic effect of NK cells (ClinicalTrials.gov: NCT02141451). We reasoned that targeting ADAM17 directly in the NK cell could avoid systemic toxicities associated with off-target effects of chemical inhibitors. Using an artificial activation system (phorbol 12-myristate 13-acetate [PMA]),[24] we demonstrate that ADAM17 KO NK cells maintain significantly higher surface expression of CD16a compared with control NK cells (which received Cas9 mRNA alone) and are on par with what is observed when NK cells are pre-treated with the ADAM17 inhibitor INCB007839 (Figure 2A; Figure S3A). Surface membrane levels of CD62L, an additional target of ADAM17,[24,33] were also undiminished in activated ADAM17 KO NK cells (Figure S3B). To test whether ADAM17 KO NK cells have enhanced ADCC, we performed standard ADCC assays using the CD20-positive Burkitt's lymphoma cell line Raji. Raji cells were pre-treated with rituximab, a mAb targeting CD20. Rituximab-coated Raji cells induced cleavage of CD16a in 79.5% ± 1.3% of control NK cells, but there were no differences in CD16a cleavage in ADAM17 KO NK cells (Figure 2B; Figure S3C). Moreover, ADAM17 KO NK cells displayed a significant increase in cytotoxic degranulation based on CD107a surface expression (Figure 2C; Figure S3D) and interferon gamma (IFNγ) production (Figure 2D; Figure S3E) in response to rit-

uximab-labeled Raji lymphoma. Importantly, ADCC was significantly enhanced when using ADAM17 KO versus control NK cells based on increased apoptosis as measured by cleaved caspase-3 in rituximab-coated Raji cells (Figure 2E; Figure S3F). Taken together, these data demonstrate that genetic KO of ADAM17 in NK cells prevents CD16a shedding comparable with ADAM17 inhibitors and leads to enhanced ADCC.

As an alternative approach, we used our gene KI strategy to deliver a non-cleavable version of CD16a (CD16 S197P)[32] to the AAVS1 locus (Figure 2F). Junction PCR confirmed targeted integration (Figure 2G). Droplet digital PCR (ddPCR) was performed to quantify a rate of 74.7% ± 5.53% targeted gene KI (Figure 2H), and CD16a expression was retained in CD16a S197P-KI NK cells after stimulation with PMA/ionomycin (Figure S3G). We confirmed enhanced function of CD16a S197P-KI NK cells using the same co-culture methods described for ADAM17 KO cells. We observed retained CD16a on the cell surface (Figure 2I) and enhanced NK cell activity and target cell killing (Figures 2J–2L). Interestingly, the enhanced ADCC effect of directly targeting CD16 was less drastic than that achieved by KO of ADAM17. It is possible that this discrepancy is due to the slight difference in gene-editing efficiency (82.7% ADAM17 KO versus 74.7% CD16a KI). Alternatively, it could be due to retention of other targets of ADAM17 when CD16 S197P is utilized. This result warrants further investigation, but it is clear that altering CD16 cleavage can enhance ADCC.

### KO of PD1 Enhances NK Cell Anti-tumor Response

NK cells are also capable of target cell killing independent of ADCC, through direct interaction between activating receptors on NK cells and cell surface proteins on target cells. However, tumor cells can block this cytotoxicity by inducing NK cell inhibitory signals through cell surface protein interactions such as PD-L1:PD1.[14,15,34] We used our gene-editing method to generate PD1 KO NK cells and tested their ability to directly kill four cancer cell lines compared with control NK cells that were electroporated with Cas9 mRNA only. We selected four cancer cell lines with various expression levels of PD-L1 and PD-L2 (Figure S4A): the chronic myeloid leukemia line K562 (PD-L1 low), the acute monocytic leukemia line THP1 (PD-L1 high), the prostate carcinoma line DU145 (PD-L1 high), and the ovarian carcinoma line MA148 (PD-L1 low). In a co-culture killing assay, PD1 KO NK cells had significantly higher levels of degranulation (Figure 3A; Figure S4B) and production of IFNγ (Figure 3B; Figure S4C). Similar to our ADCC results, PD1 KO NK cells also led to increased apoptosis of target cells compared with all controls (Figure 3C; Figure S4D).

Because there are limited data on the PD1:PD-L1 axis in NK cell function, there remains some discrepancy in the field as to its importance.[3,35,36] To confirm our results were due to PD1:PD-L1 interaction, we repeated the functional assays using wild-type (WT) and PD-L1 KO K562 (PD-L1 low) and DU145 (PD-L1 high) target cells. Importantly, control NK cells display degranulation, IFNγ production, and target cell killing at the level of PD1 KO NK cells when co-cultured with PD-L1-deficient target cells (Figures 3D–3F).
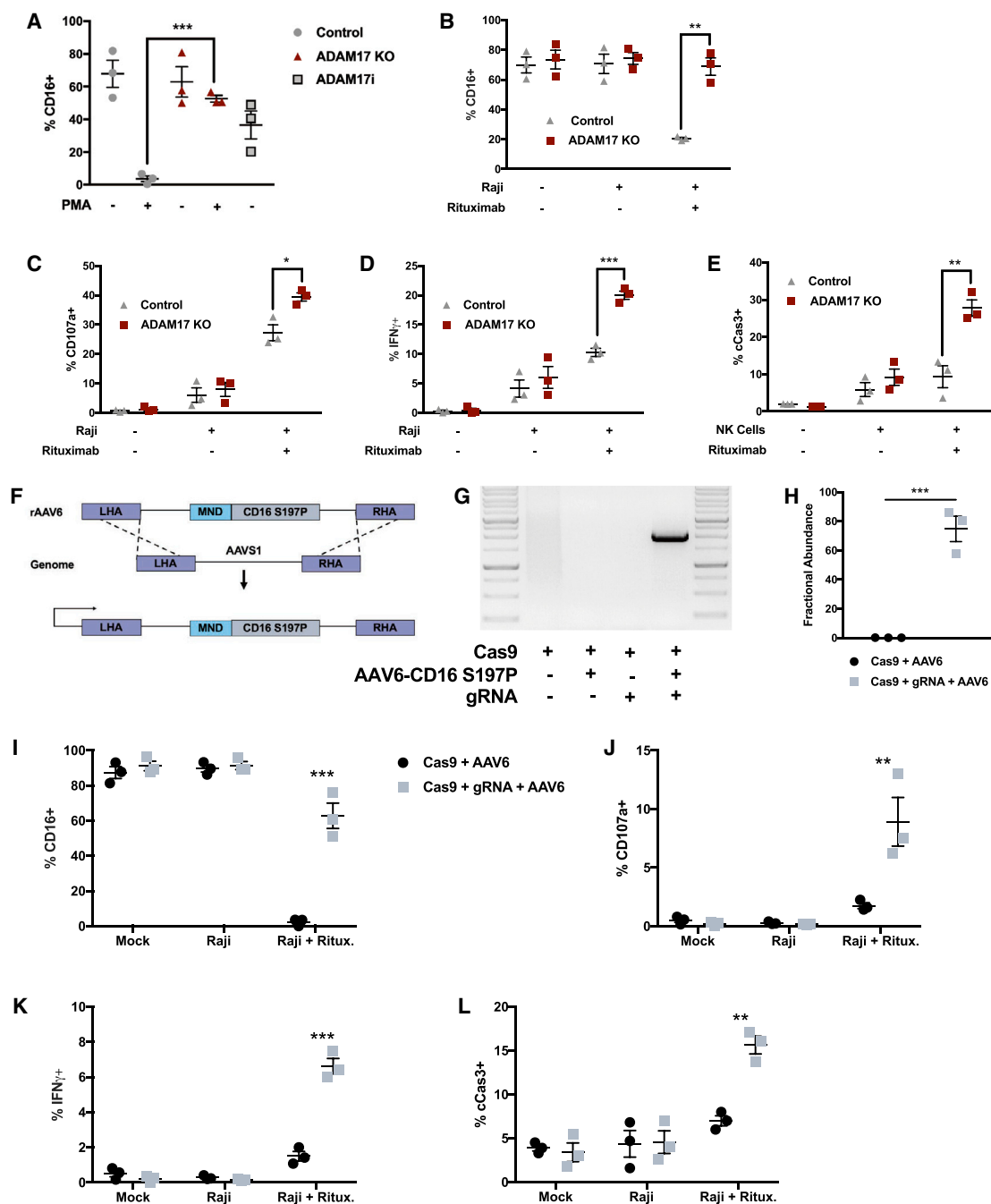
**Figure 2. ADAM17 KO and CD16 Editing Lead to Enhanced ADCC**

(A) Control NK cells were treated for 1 h with 10 μM ADAM17 inhibitor (light gray with dark outline) or DMSO (control = dark gray, ADAM17 KO = maroon). Cells were then stimulated with PMA/ionomycin (1 μg/mL) for 1 h, and CD16a expression was analyzed by flow cytometry (n = 3 independent donors, ***p = 0.0003, Student's t test). (B–E) Raji cells were labeled for 10 min with CellTrace CFSE and then incubated for 30 min with 10 μg/mL rituximab. Raji cells were then co-cultured at a 2:1 (E:T) ratio with control (dark gray) or ADAM17 KO (maroon) NK cells for 6 h (n = 3 independent donors). Flow cytometry assays detected increased NK cell CD16A expression (B) (**p = 0.0012, Student's t test), increased NK cell degranulation (C) (mock = no target cells, *p = 0.0162, Student's t test), increased NK cell IFNγ production (D) (mock = no target cells, ***p = 0.0006, Student's t test), and increased Raji cell apoptosis (E) (mock = no effector cells, **p = 0.007, Student's t test). (F) Gene knockin strategy to integrate an MND-driven non-cleavable CD16a (S197P) to the AAVS1 locus using rAAV6. (G) Primers were designed to span and amplify the 3′ junction of genomic AAVS1 and CD16. (H) Targeted knockin of MND-CD16 S197P was quantified using droplet digital PCR (n = 3 independent donors, ***p = 0.001). (I–L) CD16 S197P-KI NK cells were co-cultured with rituximab-coated Raji cells and analyzed as described above for (B)–(E) (n = 3 independent donors, **p < 0.01, ***p < 0.001, two-way ANOVA with Tukey's post hoc test).
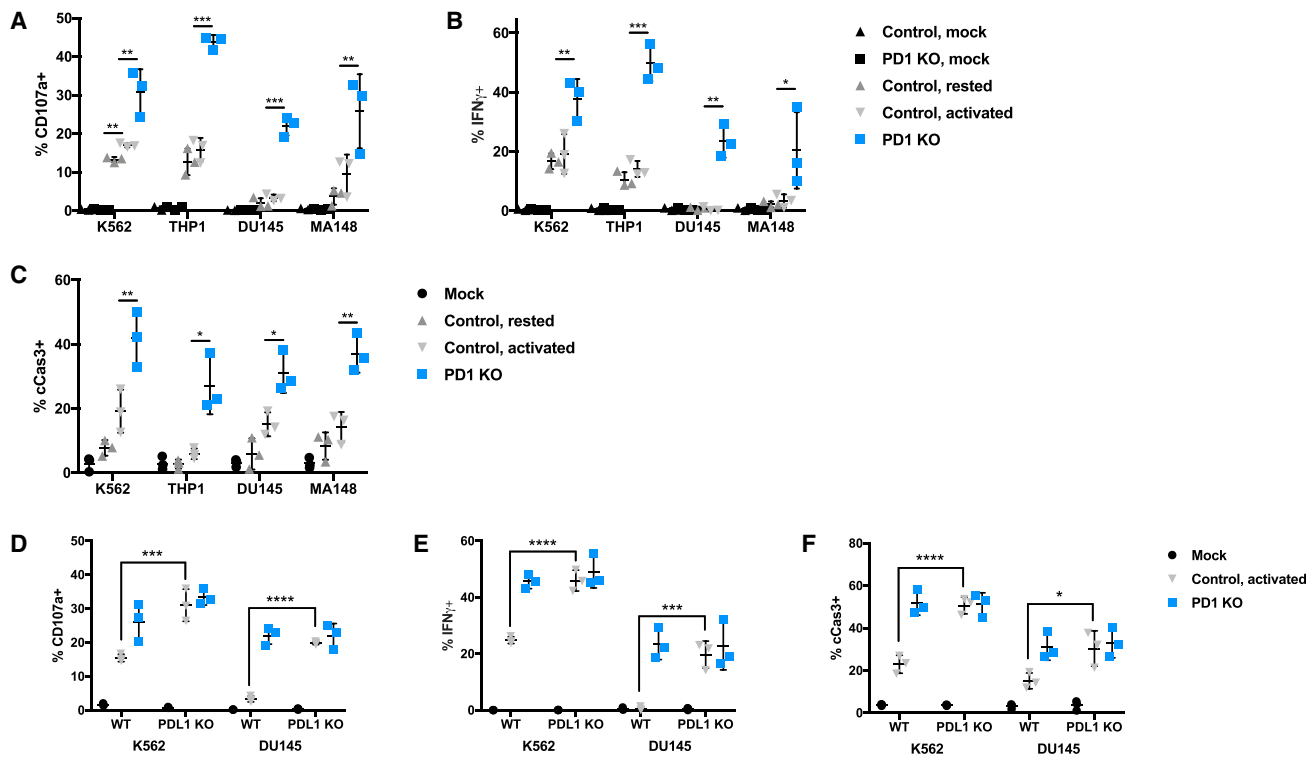
**Figure 3. PD1 KO NK Cells Demonstrate Enhanced Anti-tumor Function *In Vitro***

(A–C) Control NK cells were rested in 1 ng/mL IL-15 (light gray) to support survival as previously described.[41] Control (dark gray) and PD1 KO (blue) NK cells were activated for 1 week with C9 feeder cells. NK cells were then co-cultured at a 1:1 (E:T) ratio with target cell lines K562, THP1, DU145, and MA148 for 6 h (n = 3 independent donors, **p < 0.01, ***p < 0.001, two-way ANOVA with Tukey's post hoc test). (A) NK cell degranulation (mock = no target cells), (B) NK cell IFNγ production (mock = no target cells), and (C) target cell apoptosis (mock = no effector cells). (D–F) Control (dark gray) and PD1 KO (blue) NK cells were activated with C9 feeder cells and co-cultured at a 1:1 (E:T) ratio with wild-type (WT) or PD-L1-deficient K562 or DU145 target cells for 6 h (n = 3 independent donors, *p < 0.05, ***p < 0.001, ****p < 0.0001, two-way ANOVA with Tukey's post hoc test). (D) NK cell degranulation (mock = no target cells), (E) NK cell IFNγ production (mock = no target cells), and (F) target cell apoptosis (mock = no effector cells).

To test functionality *in vivo*, we used PD1 KO NK cells to treat an orthotopic mouse xenograft model of ovarian cancer[37] (Figure 4A). After xenograft establishment, mice were treated by a single intraperitoneal injection of rested control NK cells, donor-matched activated control NK cells that received Cas9 mRNA only, or donor-matched activated PD1 KO NK cells. Treatment with PD1 KO NK cells significantly prolonged survival (Figure 4B) and reduced tumor burden (Figure 4C) compared with both activated and rested control NK cells, indicating improved therapeutic efficacy. Supporting our hypothesis that NK cells are inhibited by PD1:PD-L1 interaction, we found that PD-L1 levels increase significantly on MA148 cells present in the ascites of mice treated with activated NK cells during tumor progression (Figure 4D). At tumor endpoint, mice were sacrificed and total ascites fluid was collected; total cells were counted and analyzed by flow cytometry. MA148 cells were identified by GFP expression, and NK cells were identified as hCD45⁺/CD56⁺. We observed higher PD-L1 expression on MA148 cells from mice treated with activated NK cells (both WT and PD1 KO) (Figure 4E). We also observed a presence of NK cells in the ascites fluid at endpoint in mice treated with activated NK cells, which was significantly higher in mice treated with PD1 KO NK cells, both as a percentage and an absolute

number (Figures 4F and 4G). These results are consistent with the hypothesis that the inflammatory environment created by activated NK cells stimulates PD-L1 expression on tumor cells and provides rationale for creating PD1-deficient NK cells for cancer therapy.

## DISCUSSION

NK cell immunotherapy holds great promise as an off-the-shelf cell therapy that does not require antigen specificity. However, the full potential of NK cell cancer therapy has not been realized, due in part to negative regulation of NK cells in the tumor microenvironment. Here we present a feasible method for generating clinical quantities of gene-edited NK cells with enhanced cytotoxic capabilities.

We chose to target two genes predicted to have a functional impact on NK cells. We were able to effectively induce efficient indel mutations in targeted genes, and gene editing was consistent across multiple independent human donors. Importantly, we show genetic changes are stable through multiple rounds of NK cell expansion, with the generation of clinical doses in a short 3-week time period. The method of expansion using C9 feeder cells has been deemed safe clinically and is currently being used in several clinical trials. We have also performed
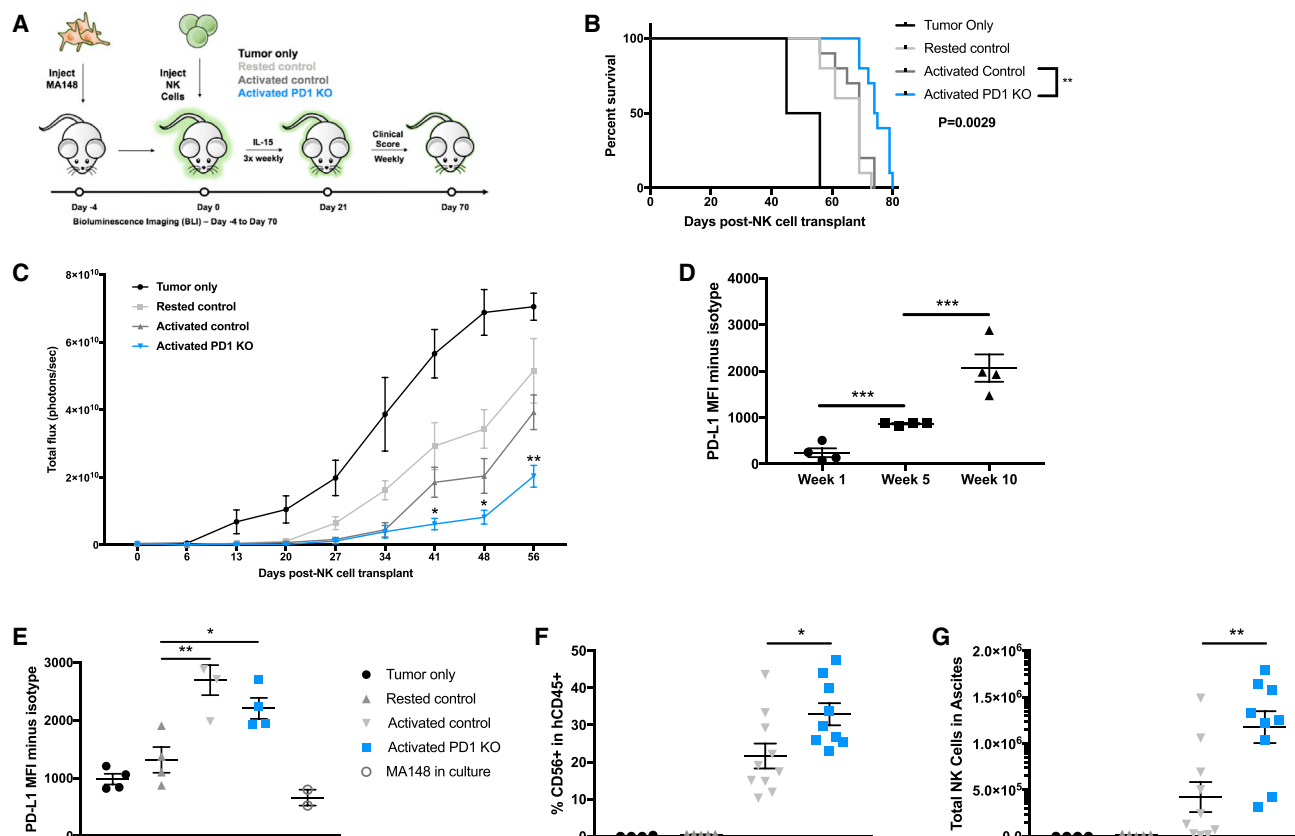
**Figure 4. PD1 KO NK Cells Demonstrate Enhanced Anti-tumor Function *In Vivo***

(A–C) A total of $2 \times 10^5$ luciferase-expressing MA148 cells were delivered i.p. to NSG mice. Four days after tumor injection, PBS (black) or $1 \times 10^6$ rested control (light gray), activated control (dark gray), or activated PD1 KO (blue) NK cells were delivered i.p. NK cells were supported with a 5 μg dose of IL-15 three times weekly for 3 weeks. Tumor burden was assessed with bioluminescence imaging weekly (n = 8–10 mice per group). (B and C) Overall survival (**p = 0.0029, log rank test) (B) and tumor burden (*p < 0.05, **p < 0.01, Student's t test) (C). (D) A subset of mice (n = 4 mice per time point) treated with activated NK cells were sacrificed at weeks 1, 5, and 10 after treatment. MA148 cells were collected from ascites via i.p. wash, and PD-L1 expression was measured by flow cytometry (***p < 0.001, Student's t test). (E–G) Ascites fluid was also collected from all treatment groups at sacrifice. Cells from the ascites were washed, enumerated, and analyzed by flow cytometry for PD-L1 expression on GFP+ MA148 cells (E) and for presence of hCD45+CD56+ NK cells (F and G) (n = 4–10 mice per group, *p < 0.05, **p < 0.01, one-way ANOVA with Tukey's post hoc test). (F) Percent CD56+ cells within hCD45+ population, and (G) total NK cells in ascites fluid based on total ascites cell count.

analyses for off-target editing across the top 10 putative off-target sites for each gRNA. We observe no detectable indel formation at any of the top 10 sites. We confirmed concurrent KO of target genes at the mRNA and protein level.

In addition to gene KO, we demonstrate efficient gene KI using rAAV6 as a template for HR. We show KI of EGFP at the AAVS1 safe harbor locus that is also stable through expansion. Beyond proof-of-principle, we have shown a functional KI of a modified non-cleavable CD16a at this locus as well. This simple method for stable gene KI provides a platform for delivery of other relevant cargo including chimeric antigen receptors (CARs) and self-stimulating cytokine receptors.

*In vitro* assays show that ADAM17 KO NK cells are more reactive to antibody-labeled target cells and are capable of enhanced killing through ADCC. These data are reiterated upon stable integration

of non-cleavable CD16a. These results are in line with previous studies using ADAM17 inhibitors, but likely come with reduced risk of unwanted off-target effects. NK cells engineered for enhanced ADCC, whether via KO of ADAM17 or modification of CD16a, will need to be tested in further *in vitro* assays using other cancer lines and mAb combinations, and in preclinical *in vivo* models.

*In vitro* and *in vivo* assays demonstrate that PD1 KO NK cells are capable of enhanced killing through non-ADCC pathways. Our data show enhanced NK cell degranulation, cytokine production, and target cell killing across a panel of tumor cell lines. There has been some discrepancy about the importance of PD-L1:PD1 interaction in NK cell function, because this axis is much more well studied in T cells than in NK cells. Using PD-L1-deficient K562 or DU145 target cells, we show that enhanced activity of PD1 KO NK cells is indeed due to PD-L1:PD1 interaction.

**Table 1. Guide RNA Target Sequences**

|  | Sequences |
|---|---|
| ADAM17 | 5′-GAACCACGCTGGTCAGGAAT-3′ |
| PD1 | 5′-CCTGCTCGTGGTGACCGAAG-3′ |
| AAVS1 | 5′-GTCACCAATCCTGTCCCTAG-3′ |
| PD-L1 | 5′-TTGAAGGACCAGCTCTCCCT-3′ |

We also delivered PD1 KO NK cells therapeutically using an *in vivo* model of ovarian cancer. Interestingly, we see upregulation of PD-L1 in these tumors upon treatment with activated NK cells, suggesting a response of the tumor cells to immune pressure. Accordingly, PD1 KO NK cells reduced tumor burden and enhanced survival in our model, and persisted at higher numbers at endpoint in the ascites fluid of tumor-bearing mice. However, despite promising functional effects *in vitro*, our *in vivo* results show only a modest improvement in survival. We suspect this is due to a need to edit multiple regulatory genes at once, because tumors can escape NK cell killing through other mechanisms, or a need for multiple infusions of NK cells.

In summary, we demonstrate an easy-to-use method for efficient gene editing in primary human NK cells. In addition, we have shown the functional consequence and therapeutic potential of KO of two genes implicated in NK cell activity. Using these optimized methods, future work will focus on editing multiple genes simultaneously, along with delivery of engineered receptors for enhancing NK cell immunotherapy.

## MATERIALS AND METHODS

### Donor NK Cell Isolation and Expansion
PBMCs from de-identified healthy human donors were obtained by automated leukapheresis (Memorial Blood Centers, Minneapolis, MN, USA) and further isolated on a Ficoll-Hypaque (Lonza) gradient. CD56^{+}CD3^{−} NK cells were isolated by negative selection using the EasySep Human NK Cell Enrichment Kit (STEMCELL Technologies). After isolation, NK cells were either rested by culture with 1 ng/mL IL-15, or activated by co-culture with C9 at a 2:1 or 1:1 (feeder/NK) ratio in B0 medium supplemented with 50 IU/mL IL-2 (PeproTech), as described previously.[21] Samples were obtained after informed consent with approval from the University of Minnesota Institutional Review Board (IRB 1602E84302).

### Cell Culture
NK cells were maintained in B0 medium[38] supplemented with 1 ng/mL IL-15 unless otherwise noted. NK cells were cryopreserved at $1 \times 10^7$ cells/mL in CryoStor CS10 (Sigma-Aldrich). The transgenic C9 cell line, the human Burkitt's lymphoma cell line Raji, the human erythroleukemia cell line K562, the human prostate cancer cell line DU145, and the human monocytic leukemia cell line THP1 were maintained in RPMI 1640 (GE Healthcare Life Sciences) supplemented with 10% fetal bovine serum (FBS; GE Healthcare Life Sciences) and 100 U/mL penicillin (Corning) and 100 U/mL streptomycin (Corning). The human ovarian cancer cell line MA148 was maintained in DMEM (GE Healthcare Life Sciences) supplemented with 10% FBS and 100 U/mL penicillin and 100 U/mL streptomycin. Cell lines were authenticated by the University of Arizona Genetics Core (UAGC) using short tandem repeat profiling. All cell lines were routinely tested for mycoplasma contamination (Lonza) and were found to be negative.

### gRNA Design
gRNAs targeting ADAM17, PD1, AAVS1, and PD-L1 were designed using the CRISPR MIT webtool (https://login.ezp1.lib.umn.edu/login?qurl=http://crispr.mit.edu%2f) along with Cas-OFFinder. Six gRNAs per target gene were tested in HEK293T cells, and the most efficient gRNA (Table 1) was purchased from TriLink Biotechnologies or Synthego with 2′-O-methyl and 3′ phosphorothioate modifications to the first three 5′ and the last three 3′ nucleotides.

### Electroporation of Activated NK Cells
Activated NK cells were pelleted and resuspended at $3 \times 10^7$ cells/mL in T buffer (Neon Transfection System Kit; Thermo Fisher Scientific). 1.5 μg Cas9 mRNA (Trilink) and 1 μg chemically modified gRNA (Trilink or Synthego) were added to 10 μL ($3 \times 10^5$ cells) on ice. Cas9 mRNA alone, without gRNA, was used as a control for all experiments. This mixture was electroporated with the Neon Transfection System (Thermo Fisher Scientific) using two pulses of 1,850 V and 10-ms pulse width. NK cells were recovered in warm B0 medium containing 1 ng/mL IL-15. For rAAV6 infection, rAAV6 (MOI = 500,000) was added to NK cells 30 min after electroporation. rAAV6 particles were produced by the University of Minnesota Vector Core and Vigene Biosciences.

### Analysis of Gene-Editing Efficiency
PCR primers were designed to amplify a 400- to 500-bp region surrounding the gRNA target site (Table 2). Five days after electroporation, genomic DNA was PCR amplified using AccuPrime Taq DNA Polymerase (Invitrogen). For analysis by TIDE, PCR amplicons were Sanger sequenced (ACGT or University of Minnesota Genomics Center), and Sanger chromatograms were uploaded to the TIDE webtool (https://www.deskgen.com/landing/tide.html). For next generation sequencing (NGS), primers with Nextera universal primer adaptors (Illumina) were designed to amplify a 350- to 475-bp site surrounding the region of interest (Table 2). Samples were submitted to the University of Minnesota Genomics Center for subsequent amplification with indexing primers and sequencing on a MiSeq 2×200 bp run (Illumina). A minimum of 1,000 read-pairs were generated per sample. Raw .fastq files were analyzed against a reference sequence and gRNA protospacer sequence using the CRISPR/Cas9 editing analysis pipeline CRISPR-DAV, as previously described.[39]

### ddPCR
Targeted integration of MND-CD16 at AAVS1 was quantified using ddPCR. Assays were designed using PrimerQuest software (Integrated DNA Technologies) using settings for two primers + probe qPCR. Each sample was run as a duplexed assay consisting of an

**Table 2. Primer Sequences**

| Primer Name | Forward | Reverse |
|---|---|---|
| ADAM17 PCR | 5′-cccgatgtgagcagttttcc-3′ | 5′-gagacaggcccatctccttt-3′ |
| PD1 PCR | 5′-gggtgaaggctcttagtagg-3′ | 5′-caggctctctttgatctgc-3′ |
| AAVS1 PCR | 5′-ACTCCTTTCATTTGGGCAGC-3′ | 5′-GGTTCTGGCAAGGAGAGAGA-3′ |
| ADAM17 NGS | 5′-TCGTCGGCAGCGTCAGATGTGTATAAGAGACAGCGGTAGAATCTTCCCAGTAG-3′ | 5′-GTCTCGTGGGCTCGGAGATGTGTATAAGAGACAGCCCAAACACCTGATAGACC-3′ |
| PD1 NGS | 5′-TCGTCGGCAGCGTCAGATGTGTATAAGAGACAGCACCTCTCTCCATCTCTCAG-3′ | 5′-GTCTCGTGGGCTCGGAGATGTGTATAAGAGACAGCAGGCTCTCTTTGATCTGC-3′ |
| ADAM17 RT-PCR | 5′-ACCTGAAGAGCTTGTTCATCGAG-3′ | 5′-CCATGAAGTGTTCCGATAGATGTC-3′ |
| PD1 RT-PCR | 5′-ACCTGGGTGTTGGGAGGGCA-3′ | 5′-GGAGTGGATAGGCCACGGCG-3′ |
| β-Actin RT-PCR | 5′-CACAGGGGGAGGTGATAGCAT-3′ | 5′-CTCAAGTTGGGGGACAAAAA-3′ |
| AAVS1-GFP Jxn PCR | 5′-GGACGAGCTGTACAAGTAACG-3′ | 5′-GAGACAGTGACCAACCATCC-3′ |
| AAVS1-CD16 Jxn PCR | 5′-TCTTGAGGGTCCTTTCTCCA-3′ | 5′-CTCTGTTCAGCCCTAAGAATCC-3′ |

internal reference primer + probe set (HEX) and an experimental primer + probe set (FAM) (Table 3). Reactions were set up in duplicate using the ddPCR Supermix for Probes (Bio-Rad) with 50 ng genomic DNA per assay according to the manufacturer's instructions. Droplets were generated and analyzed using the QX200 Droplet Digital PCR system (Bio-Rad).

## qRT-PCR
RNA was extracted using the PureLink RNA Mini Kit (Ambion). cDNA was generated using the Transcriptor First Strand cDNA Synthesis Kit (Roche). Real-time PCR was conducted using exon-exon junction primer sets (Table 2) and SYBR Green Master Mix (Applied Biosystems), and analyzed using a CFX-96 (Bio-Rad). Gene expression levels were calculated relative to β-actin and expressed as a fold change compared with control.

## Antibodies and Flow Cytometry
The following antibodies were used: allophycocyanin (APC)-, fluorescein isothiocyanate (FITC)-, phycoerythrin (PE)-, or biotin-conjugated anti-CD56 (clone REA196; Miltenyi Biotec), PE-conjugated anti-CD3 (clone SK7; BD Biosciences), PE/Cy7-conjugated anti-CD16A (clone 3G8; BioLegend), Brilliant Violet 421-conjugated anti-CD16A (clone 3G8; BioLegend), Brilliant UV 395-conjugated anti-CD158b (BD Biosciences), PE-conjugated anti-CD336 (clone P44-8.1; BD Biosciences), Brilliant Violet 421-conjugated anti-CD337 (clone P30; BD Biosciences), FITC-conjugated anti-NKB1 (clone DX9; BD Biosciences), PE-Cy7-conjugated anti-CD314 (clone 1D11; BD Biosciences), APC-conjugated anti-NKp46 (clone 9E2; BD Biosciences), FITC-conjugated anti-CD226 (clone DX11; BD Biosciences), Brilliant Violet 421-conjugated anti-IFNγ (clone 4S.B3; BioLegend), FITC-conjugated anti-CD107a (clone H4A3; BD Biosciences), Brilliant Violet 605-conjugated anti-CD62L (clone Dreg56; BD Biosciences), PE-conjugated anti-active caspase-3 (clone C92-605; BD Biosciences), SYTOX Blue dead cell stain (Thermo Fisher),

and fixable viability dye eFluor 780 (eBioscience). Detection of ADAM17 was performed using anti-hTACE ectodomain (R&D Systems) followed by biotinylated anti-mouse IgG (R&D Systems) and Brilliant Violet 421-labeled streptavidin (BioLegend). Detection of PD1 was performed using optimized mild acid treatment followed by staining with PE-labeled anti-PD1 (clone PD1.3.1.3; Miltenyi Biotec). Flow cytometry assays were performed on LSRII or LSR Fortessa flow cytometers (BD Biosciences), and all data were analyzed with FlowJo version 10.4 software (FlowJo).

## NK Cell Functional Assays
For PMA stimulation, NK cells were pre-treated for 1 h with 10 μM ADAM17 inhibitor (INCB007839) or DMSO control. NK cells were then stimulated with 1 μg/mL PMA for 1 h, and CD16a expression was measured by flow cytometry. For intracellular cytokine staining, NK cells were plated at $2.5 \times 10^5$ cells per 100 μL B0 with no cytokines added. After incubation overnight, target cells were added at the indicated E:T ratios (2:1 for assays with ADAM17 KO NK cells, 1:1 for assays with PD1 KO NK cells). For ADCC assays, Raji cells were pre-coated with rituximab (Genentech) at 10 μg/mL for 30 min. FITC-conjugated anti-CD107a was added to the culture, and cells were incubated for 1 h at 37°C. Brefeldin A and monensin (BD Biosciences) were added after 1 h, and cells were incubated for an additional 5 h. Cells were stained with fixable viability dye and for extracellular antigens and then were fixed and permeabilized using BD Cytofix/Cytoperm (BD Biosciences). Cells were then stained for intracellular IFNγ.

## Target Cell Killing Assays
NK cells were plated at $2.5 \times 10^5$ cells per 100 μL B0 medium with no cytokines added, and incubated overnight. Target cells were pelleted and labeled with CellTrace CFSE (Thermo Fisher Scientific) for 10 min at room temperature, then washed in 10 mL FBS. For ADCC assays, CFSE-labeled Raji cells were pre-coated with rituximab

**Table 3. ddPCR Sequences**

|  | Assay | Sequences |
|---|---|---|
| MND-AAVS1 forward | experimental | 5′-CTGAAATGACC CTGTGCCTTAT-3′ |
| MND-AAVS1 reverse | experimental | 5′-GCGATCTGACG GTTCACTAAA-3′ |
| MND-AAVS1 probe | experimental (FAM) | 5′-ACCAATCAGTT CGCTTCTCGCTTCT-3′ |
| B2M exon 3 forward | reference | 5′-GGTTTCATCCAT CCGACATTGAAGT TGAC-3′ |
| B2M exon 3 reverse | reference | 5′-GGGTGAATTCAG TGTAGTACAAGAG ATAG-3′ |
| B2M exon 3 probe | reference (HEX) | 5′-GACCAGTCCTTG CTGAAAGACAAG TCTG-3′ |

(Genentech) at 10 μg/mL for 30 min. CFSE-labeled target cells were added to NK cells (E:T = 2:1 for ADAM17 assays, E:T = 1:1 for PD1 assays). Co-cultures were incubated at 37°C for 6 h. Cells were stained with fixable viability dye and then were fixed and permeabilized with ice-cold 70% ethanol for 30 min. Cells were then stained for active caspase-3.

### *In Vivo* Tumor Model

All animal studies were approved by the University of Minnesota Institutional Animal Care and Use Committee (IACUC 1610-34201A). Non-obese diabetic (NOD)/severe combined immunodeficiency (SCID)/$\gamma c^{-/-}$ (NSG) mice were purchased from Jackson Laboratories and used for all *in vivo* experiments. Mice were given $2 \times 10^5$ luciferase-expressing MA148 ovarian carcinoma cells[37,40] via intraperitoneal (i.p.) injection 4 days prior to NK cell delivery. One day before NK cell treatment, mice were sub-lethally irradiated (225 cGy), and tumor burden was measured by bioluminescent imaging (BLI) using the Xenogen IVIS 50 Imaging System (Caliper Life Sciences). Mice were then grouped based on BLI to ensure each treatment group started with the same average tumor burden. On day 0, NK cells ($1 \times 10^6$ cells per mouse) were delivered i.p. BLI was measured weekly. Mice received i.p. injections of IL-15 (5 μg/mouse) every Monday, Wednesday, and Friday for 3 weeks. Animal health was monitored daily, and mice were euthanized when moribund. Upon sacrifice, ascites fluid was collected by i.p. wash. Cells in the ascites fluid were washed, enumerated, and stained for flow cytometry for hCD45, CD56, CD3, and PD-L1. Total NK cells in ascites fluid were calculated by applying percent $hCD54^+CD56^+$ to the total ascites cell count.

### Predicted Off-Target Analysis and Next Generation Sequencing

Putative off-target sites were predicted for each gRNA using the offTargetAnalysis function from the CRISPRseek R package (version 3.8, PMID: 25247697) using University of California Santa Cruz (UCSC) hg19 and a maximum mismatch number of 4. Primers with Nextera universal primer adaptors (Illumina) were designed to amplify a 350-475-bp site surrounding either the on-target (OnT) or off-target (OT) region of interest using Primer3Plus (http://bioinfo.ut.ee/primer3-0.4.0/). Genomic DNA was PCR amplified using AccuPrime Taq DNA polymerase according to the manufacturer's protocol (Invitrogen). Samples were run on a 1% agarose gel and gel extracted using QIAquick Gel Extraction Kit (QIAGEN). Samples were submitted to the University of Minnesota Genomics Center for subsequent amplification with indexing primers and sequencing on a MiSeq 2×300-bp run (Illumina). A minimum of 1,000 read-pairs were generated per OnT sample and 10,000 read-pairs per OT sample. Raw fastq files were analyzed against a reference sequence and gRNA protospacer sequence using the CRISPR/Cas9 editing analysis pipeline CRISPR-DAV as previously described.[39] Output "sample_snp.xlsx" and "sample_len.xlsx" were compiled and analyzed using a custom R markdown script (RStudio v1.1.383, R v3.4.2). Raw .fastq files and custom script will be made available upon request.

### Statistical Analysis

The Student's t test was used to test for significant differences between two groups. Differences between three or more groups were tested by one-way ANOVA followed by Tukey's post hoc test. All *in vitro* assays were repeated in three to five independent donors. Mean values ± SEM are shown. The level of significance was set at α = 0.05. Statistical analyses were performed using GraphPad Prism 7.0.

### SUPPLEMENTAL INFORMATION

Supplemental Information can be found online at https://doi.org/10.1016/j.ymthe.2019.10.009.

# REFERENCES

1. Murphy, W.J., Parham, P., and Miller, J.S.N.K. (2012). NK cells—from bench to clinic. Biol. Blood Marrow Transplant. 18 (Suppl 1), S2–S7.

2. Davis, Z.B., Felices, M., Verneris, M.R., and Miller, J.S. (2015). Natural Killer Cell Adoptive Transfer Therapy: Exploiting the First Line of Defense Against Cancer. Cancer J. 21, 486–491.

3. Davis, Z.B., Vallera, D.A., Miller, J.S., and Felices, M. (2017). Natural killer cells unleashed: Checkpoint receptor blockade and BiKE/TriKE utilization in NK-mediated anti-tumor immunotherapy. Semin. Immunol. 31, 64–75.

4. Podgorny, P.J., Liu, Y., Dharmani-Khan, P., Pratt, L.M., Jamani, K., Luider, J., Auer-Grzesiak, I., Mansoor, A., Williamson, T.S., Ugarte-Torres, A., et al. (2014). Immune cell subset counts associated with graft-versus-host disease. Biol. Blood Marrow Transplant. 20, 450–462.

5. Knorr, D.A., Bachanova, V., Verneris, M.R., and Miller, J.S. (2014). Clinical utility of natural killer cells in cancer therapy and transplantation. Semin. Immunol. 26, 161–172.

6. Schmiedel, D., Tai, J., Yamin, R., Berhani, O., Bauman, Y., and Mandelboim, O. (2016). The RNA binding protein IMP3 facilitates tumor immune escape by downregulating the stress-induced ligands ULPB2 and MICB. eLife 5, e13426.

7. Hofer, E., and Koehl, U. (2017). Natural Killer Cell-Based Cancer Immunotherapies: From Immune Evasion to Promising Targeted Cellular Therapies. Front. Immunol. 8, 745.

8. Chester, C., Fritsch, K., and Kohrt, H.E. (2015). Natural Killer Cell Immunomodulation: Targeting Activating, Inhibitory, and Co-stimulatory Receptor Signaling for Cancer Immunotherapy. Front. Immunol. 6, 601.

9. Keating, G.M. (2010). Rituximab: a review of its use in chronic lymphocytic leukaemia, low-grade or follicular lymphoma and diffuse large B-cell lymphoma. Drugs 70, 1445–1476.

10. Ahlgrimm, M., Pfreundschuh, M., Kreuz, M., Regitz, E., Preuss, K.D., and Bittenbring, J. (2011). The impact of Fc-γ receptor polymorphisms in elderly patients with diffuse large B-cell lymphoma treated with CHOP with or without rituximab. Blood 118, 4657–4662.

11. Wu, J., Mishra, H.K., and Walcheck, B. (2019). Role of ADAM17 as a regulatory checkpoint of CD16A in NK cells and as a potential target for cancer immunotherapy. J. Leukoc. Biol 105, 1297–1303.

12. Mishra, H.K., Pore, N., Michelotti, E.F., and Walcheck, B. (2018). Anti-ADAM17 monoclonal antibody MEDI3622 increases IFNγ production by human NK cells in the presence of antibody-bound tumor cells. Cancer Immunol. Immunother. 67, 1407–1416.

13. Vitale, M., Cantoni, C., Pietra, G., Mingari, M.C., and Moretta, L. (2014). Effect of tumor cells and tumor microenvironment on NK-cell function. Eur. J. Immunol. 44, 1582–1592.

14. Guo, Y., Feng, X., Jiang, Y., Shi, X., Xing, X., Liu, X., Li, N., Fadeel, B., and Zheng, C. (2016). PD1 blockade enhances cytotoxicity of in vitro expanded natural killer cells towards myeloma cells. Oncotarget 7, 48360–48374.

15. Ray, A., Das, D.S., Song, Y., Richardson, P., Munshi, N.C., Chauhan, D., and Anderson, K.C. (2015). Targeting PD1-PDL1 immune checkpoint in plasmacytoid dendritic cell interactions with T cells, natural killer cells and multiple myeloma cells. Leukemia 29, 1441–1444.

16. Vey, N., Bourhis, J.H., Boissel, N., Bordessoule, D., Prebet, T., Charbonnier, A., Etienne, A., Andre, P., Romagne, F., Benson, D., et al. (2012). A phase 1 trial of the anti-inhibitory KIR mAb IPH2101 for AML in complete remission. Blood 120, 4317–4323.

17. Chan, C.J., Martinet, L., Gilfillan, S., Souza-Fonseca-Guimaraes, F., Chow, M.T., Town, L., Ritchie, D.S., Colonna, M., Andrews, D.M., and Smyth, M.J. (2014). The receptors CD96 and CD226 oppose each other in the regulation of natural killer cell functions. Nat. Immunol 15, 431–438.

18. Lesokhin, A.M., Callahan, M.K., Postow, M.A., and Wolchok, J.D. (2015). On being less tolerant: Enhanced cancer immunosurveillance enabled by targeting checkpoints and agonists of T cell activation. Sci. Transl. Med 7, 280sr1.

19. Osborn, M.J., Webber, B.R., Knipping, F., Lonetree, C.L., Tennis, N., DeFeo, A.P., McElroy, A.N., Starker, C.G., Lee, C., Merkel, S., et al. (2016). Evaluation of TCR Gene Editing Achieved by TALENs, CRISPR/Cas9, and megaTAL Nucleases. Mol. Ther. 24, 570–581.

20. Johnson, M.J., Laoharawee, K., Lahr, W.S., Webber, B.R., and Moriarity, B.S. (2018). Engineering of Primary Human B cells with CRISPR/Cas9 Targeted Nuclease. Sci. Rep. 8, 12144.

21. Denman, C.J., Senyukov, V.V., Somanchi, S.S., Phatarpekar, P.V., Kopp, L.M., Johnson, J.L., Singh, H., Hurton, L., Maiti, S.N., Huls, M.H., et al. (2012). Membrane-bound IL-21 promotes sustained ex vivo proliferation of human natural killer cells. PLoS ONE 7, e30264.

22. Shah, N., Li, L., McCarty, J., Kaur, I., Yvon, E., Shaim, H., Muftuoglu, M., Liu, E., Orlowski, R.Z., Cooper, L., et al. (2017). Phase I study of cord blood-derived natural killer cells combined with autologous stem cell transplantation in multiple myeloma. Br. J. Haematol. 177, 457–466.

23. Hendel, A., Bak, R.O., Clark, J.T., Kennedy, A.B., Ryan, D.E., Roy, S., Steinfeld, I., Lunstad, B.D., Kaiser, R.J., Wilkens, A.B., et al. (2015). Chemically modified guide RNAs enhance CRISPR-Cas genome editing in human primary cells. Nat. Biotechnol 33, 985–989.

24. Romee, R., Foley, B., Lenvik, T., Wang, Y., Zhang, B., Ankarlo, D., Luo, X., Cooley, S., Verneris, M., Walcheck, B., and Miller, J. (2013). NK cell CD16 surface expression and function is regulated by a disintegrin and metalloprotease-17 (ADAM17). Blood 121, 3599–3608.

25. Jensen, K.T., Fløe, L., Petersen, T.S., Huang, J., Xu, F., Bolund, L., Luo, Y., and Lin, L. (2017). Chromatin accessibility and guide sequence secondary structure affect CRISPR-Cas9 gene editing efficiency. FEBS Lett. 591, 1892–1901.

26. Brinkman, E.K., Chen, T., Amendola, M., and van Steensel, B. (2014). Easy quantitative assessment of genome editing by sequence trace decomposition. Nucleic Acids Res. 42, e168.

27. Sentmanat, M.F., Peters, S.T., Florian, C.P., Connelly, J.P., and Pruett-Miller, S.M. (2018). A Survey of Validation Strategies for CRISPR-Cas9 Editing. Sci. Rep. 8, 888.

28. Veluchamy, J.P., Kok, N., van der Vliet, H.J., Verheul, H.M.W., de Gruijl, T.D., and Spanholtz, J. (2017). The Rise of Allogeneic Natural Killer Cells As a Platform for Cancer Immunotherapy: Recent Innovations and Future Developments. Front. Immunol. 8, 631.

29. Lapteva, N., Szmania, S.M., van Rhee, F., and Rooney, C.M. (2014). Clinical grade purification and expansion of natural killer cells. Crit. Rev. Oncog. 19, 121–132.

30. Bak, R.O., and Porteus, M.H. (2017). CRISPR-Mediated Integration of Large Gene Cassettes Using AAV Donor Vectors. Cell Rep. 20, 750–756.

31. Bak, R.O., Dever, D.P., and Porteus, M.H. (2018). CRISPR/Cas9 genome editing in human hematopoietic stem cells. Nat. Protoc. 13, 358–376.

32. Jing, Y., Ni, Z., Wu, J., Higgins, L., Markowski, T.W., Kaufman, D.S., and Walcheck, B. (2015). Identification of an ADAM17 cleavage region in human CD16 (FcγRIII) and the engineering of a non-cleavable version of the receptor in NK cells. PLoS ONE 10, e0121788.

33. Li, Y., Brazzell, J., Herrera, A., and Walcheck, B. (2006). ADAM17 deficiency by mature neutrophils has differential effects on L-selectin shedding. Blood 108, 2275–2279.

34. Hsu, J., Hodgins, J.J., Marathe, M., Nicolai, C.J., Bourgeois-Daigneault, M.C., Trevino, T.N., Azimi, C.S., Scheer, A.K., Randolph, H.E., Thompson, T.W., et al. (2018). Contribution of NK cells to immunotherapy mediated by PD-1/PD-L1 blockade. J. Clin. Invest. *128*, 4654–4668.

35. Mazzaschi, G., Facchinetti, F., Missale, G., Canetti, D., Madeddu, D., Zecca, A., Veneziani, M., Gelsomino, F., Goldoni, M., Buti, S., et al. (2019). The circulating pool of functionally competent NK and CD8+ cells predicts the outcome of anti-PD1 treatment in advanced NSCLC. Lung Cancer *127*, 153–163.

36. Del Zotto, G., Marcenaro, E., Vacca, P., Sivori, S., Pende, D., Della Chiesa, M., Moretta, F., Ingegnere, T., Mingari, M.C., Moretta, A., and Moretta, L. (2017). Markers and function of human NK cells in normal and pathological conditions. Cytometry B Clin. Cytom. *92*, 100–114.

37. Felices, M., Chu, S., Kodal, B., Bendzick, L., Ryan, C., Lenvik, A.J., Boylan, K.L.M., Wong, H.C., Skubitz, A.P.N., Miller, J.S., and Geller, M.A. (2017). IL-15 super-agonist (ALT-803) enhances natural killer (NK) cell function against ovarian cancer. Gynecol. Oncol. *145*, 453–461.

38. Pierson, B.A., McGlave, P.B., Hu, W.S., and Miller, J.S. (1995). Natural killer cell proliferation is dependent on human serum and markedly increased utilizing an enriched supplemented basal medium. J. Hematother. *4*, 149–158.

39. Wang, X., Tilford, C., Neuhaus, I., Mintier, G., Guo, Q., Feder, J.N., and Kirov, S. (2017). CRISPR-DAV: CRISPR NGS data analysis and visualization pipeline. Bioinformatics *33*, 3811–3812.

40. Yokoyama, Y., Dhanabal, M., Griffioen, A.W., Sukhatme, V.P., and Ramakrishnan, S. (2000). Synergy between angiostatin and endostatin: inhibition of ovarian cancer growth. Cancer Res. *60*, 2190–2196.

41. Romee, R., Schneider, S.E., Leong, J.W., Chase, J.M., Keppel, C.R., Sullivan, R.P., Cooper, M.A., and Fehniger, T.A. (2012). Cytokine activation induces human memory-like NK cells. Blood *120*, 4751–4760.